Synthesis and characterization of $La_{0.75}Sr_{0.25}Cr_{0.5}Mn_{0.5}O_{3-\delta}$ nanoparticles using a combustion method for solid oxide fuel cells

V S Reddy Channu[*], Rudolf Holze[*], Edwin H. Walker,Jr[**], Rajamohan R. Kalluru[***]

[*] Institut für Chemie, AG Elektrochemie, Technische Universität Chemnitz, D-09107 Chemnitz, Germany, subbu5reddy@yahoo.co.in

[**]Department of Chemistry, Southern University and A&M College, P.O. Box 12566, Baton Rouge, LA 70813,USA

[***]KITE College of Professional Engineering Sciences, Jawaharlal Nehru Technological University of Hyderabad, Shabad-509217, India

ABSTRACT

$La_{0.75}Sr_{0.25}Cr_{0.5}Mn_{0.5}O_{3-\delta}$ (LSCM) perovskite nanoparticles for use as anode material in intermediate temperature solid oxide fuel cells (IT-SOFCs) were synthesized using 3,3',3"- nitrilotripropionic acid (NTP), citric acid and oxalic acid as carriers via a combustion method. The influence of the carrier on phase and morphology of the obtained pristine products was characterized using X-ray diffraction (XRD), thermal gravimetric analysis (TGA), and scanning electron microscopy (SEM). XRD results showed, that the LSCM had rhombohedral symmetry with R-3c space group; a single phase LSCM perovskite formed after calcination of fired gel at 1200 °C for 7 h. Scanning electron microscopy analysis of the pristine powders showed spherical shape and particle sizes in the range of 50 – 500 nm.

Keywords: Nanoparticles; Combustion method; Morphology; Carriers

1 INTRODUCTION

A fuel cell is an electrochemical device that converts chemical energy of fuels (hydrogen, methane, butane or even gasoline and diesel) into electrical energy by exploiting the natural tendency of oxygen and hydrogen to react. Fuel cells are simple devices containing no moving parts and only four functional components namely cathode, electrolyte, anode and interconnect. Solid oxide fuel cells (SOFCs) are considered to be among the most versatile power production facilities. Their unique characteristics include extreme efficiency, significant energy conversion rate with a wide range of fuels and pollution-free operation. On the other hand high operating temperature (about 1000 ºC) of the SOFC results in problems including difficult sealing between cells with flat plate configurations and thermal expansion mismatches between components. In addition, the high operating temperature places rigorous constraints on materials selection and results in difficult fabrication processes [1].

Recently, perovskite based conducting oxides, such as substituted lanthanum chromites or lanthanum manganates and strontium titanates, received great attention as alternative anode materials for solid oxide fuel cells [2]. Particularly, $(La_{0.75}Sr_{0.25})_{1-x}Cr_{0.5}Mn_{0.5}O_{3-\delta}$ perovskite phase (LSCM) has been considered as a capable anode material for SOFCs due to its electrocatalytic/catalytic activity for oxidation of methane fuel in the absence of steam, reduced carbon deposition, and high durability against sulfur poisoning and good electrical properties [3, 4]. Predominantly, this composition of LSCM has shown good stability in fuels and in air, and has good resistance towards carbon deposition and low polarization resistance when used with hydrocarbon fuels [5]. LSCM can also be used as a cathode, thus facilitating fuel cells with a symmetrical structure (LSCM/electrolyte/LSCM) [6, 7].

Up till now, various chemical methods were reported in the literature for the synthesis of LSCM powders, for example, glycine nitrate method [3], EDTA (ethylenediaminetetraacetic acid) chelating method [8,9], combustion synthesis [7,10], solid-state reaction [4, 6, 11 – 15], gel-casting [16, 17] and co-precipitation method [18]. The solid-state method has some disadvantages such as high temperature (above 1300 ºC) and long duration of synthesis of LSCM and non-homogeneity in particle size and low purity [19]. However, to synthesize homogeneous fine particles of pure phase LSCM powders requires low temperature and short duration of synthesis. The solution combustion method is suitable to synthesize nanosize LSCM particles with good homogeneity [20]. The present work reports on the synthesis of nanostructured $La_{0.75}Sr_{0.25}Cr_{0.5}Mn_{0.5}O_{3-\delta}$ (LSCM) perovskite by a combustion method using 3,3',3"- nitrilotripropionic acid, oxalic acid and citric acid as carriers.

2 EXPERIMENTAL

Nanostructured $La_{0.75}Sr_{0.25}Cr_{0.5}Mn_{0.5}O_{3-\delta}$ (LSCM) perovskite anode material was synthesized by a combustion technique. Three batches of LSCM solutions are prepared with stoichiometric amounts of lanthanum nitrate ($La(NO_3)_3{\cdot}6H_2O$), strontium nitrate ($Sr(NO_3)_2$), chromium nitrate ($Cr(NO_3)_3{\cdot}9H_2O$) and manganese nitrate ($Mn(NO_3)_2$) in distilled water under constant stirring. First, a stoichiometric amount of citric acid ($C_6H_8O_7{\cdot}H_2O$) and 15 mL ethylene glycol, second, oxalic acid and 15 mL ethylene glycol, and 3,3',3"- nitrilotripropionic acid and 15mL ethylene glycol which are chelating agents and fuel, were also dissolved in LSCM solution. The stoichiometric ratio of carriers to nitrates was 2 [21]. A gel was formed with continuous stirring and mild heating at 120 °C. The gel was dried at room temperature for overnight and then heated at 350 ºC for 30 min. The resulting powders were ground in an agate mortar and heated in air at 1000 ºC for 7 h. Finally, the ground product was heated at 1200 ºC for 7 h in air.

Crystallographic information of the samples was obtained using an X-ray powder diffractometer (D8 Advanced Brucker) with graphite monochromatized Cu Kα radiation (λ = 1.54187 Å). Diffraction data were collected over the 2θ range of 15 to 80°. The morphologies of the resulting products were characterized using a scanning electron microscope (SEM, JEOL JSM 6390). For the TGA measurements a TA 600, operating in dynamic mode (heating rate =10°C/min), was employed.

3 RESULTS AND DISCUSSION

Phase purity and crystallographic information of the synthesized $La_{0.75}Sr_{0.25}Cr_{0.5}Mn_{0.5}O_{3-\delta}$ perovskite nanoparticles were characterized using powder X-ray diffraction. The XRD patterns of LSCM perovskite nanoparticles are shown in Fig. 1. All diffraction patterns of $La_{0.75}Sr_{0.25}Cr_{0.5}Mn_{0.5}O_{3-\delta}$ perovskite nanoparticles show characteristic peaks of the perovskite phase. The XRD patterns are in good agreement with the standard data for rhombohedral symmetry with a = 5.4736 Å, b = 5.4736 Å, c = 13.2898 Å and R-3c space group (JCPDS # 01-070-8673). No impurity phases were observed presumably because in the solid-state reaction the pure phase of $La_{0.75}Sr_{0.25}Cr_{0.5}Mn_{0.5}O_{3-\delta}$ (LSCM) perovskite was formed at 1200 ºC [21]. The crystallite size of the LSCM nanoparticles was calculated using Debye–Scherrer formula at (110) plane. The size of the LSCM-particles prepared NTP-assisted is 57.65 nm, with citric acid and oxalic acid the value is 68.63 nm.

In the synthesis of $La_{0.75}Sr_{0.25}Cr_{0.5}Mn_{0.5}O_{3-\delta}$ (LSCM) perovskite nanoparticles the carriers (NTP, oxalic acid and citric acid) help in obtaining a homogeneous mixture of the cations in a solution through forming metal complexes, they also help in the reduction of nitrates in a combustion process, releasing a large amount of heat. This is shown by an exothermic peak at 377 ºC on a DSC curve (Fig. 2). During the solid-state reduction process, metal cations and oxygen anions stay in the react and mixture during the formation of perovskite phase in this combustion process. The large heat released during combustion might be of the help to overcome the lattice energy, which is required for the formation of the perovskite phase, and also the completion of the nucleation by the rearrangement of atoms by short distance diffusion. The fast combustion process might not be of help for the diffusion of atoms far from each other and hence the particle size of LSCM powder remained in the nanometer range [22].

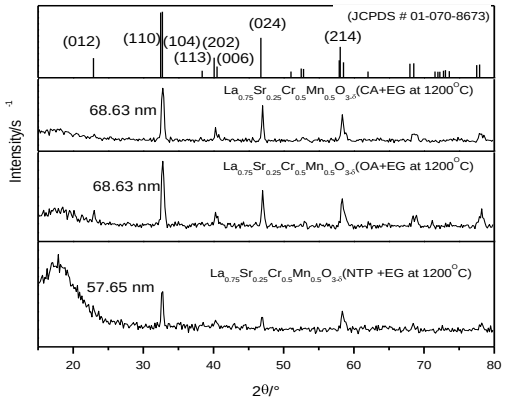

Figure 1: XRD patterns of $La_{0.75}Sr_{0.25}Cr_{0.5}Mn_{0.5}O_{3-\delta}$ (LSCM) perovskite phase nanoparticles

.

Thermogravimetric analysis and differential scanning calorimetry (TGA-DSC) curves with NTP-assisted LSCM dried as a gel at 120 ºC are shown in Fig.2. The weight losses happen in three steps. The total weight loss was 2.1 mg from room temperature to 1300 ºC. The first weight loss is 0.33 mg in the temperature range 22 - 236 °C; this can be attributed to evaporation of water from the layers of LSCM. The second weight loss is 1.25 mg in the temperature range 236 - 383 °C and the third weight loss is 0.5 mg in the temperature range 383 - 837 °C. The second and third weight losses are attributed to decomposition of the carrier (NTP) and evaporation of structurally bounded water. The peaks located at about 295 and 377 °C are exothermic on the DSC curve due to decomposition of nitrates and organic matter and correspond to the second weight loss of 1.25 mg from about 236 to 400 °C as observed in the TGA curve.

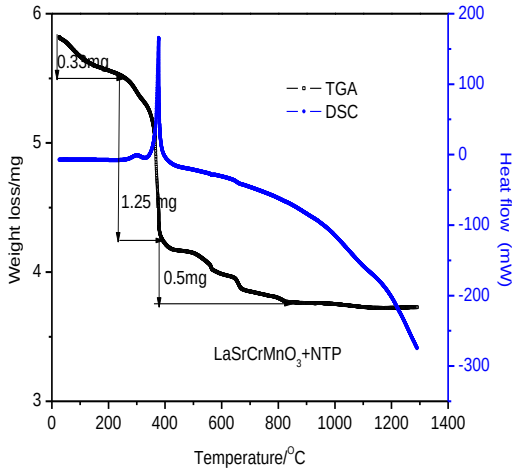

Figure 2: TGA-DSC curves of $La_{0.75}Sr_{0.25}Cr_{0.5}Mn_{0.5}O_{3-\delta}$ (LSCM) perovskite gel precursor dried at 120 ° C.

To observe thermal effects above 350 ºC, different carrier-assisted LSCM samples were fired at 350 ºC for 1 h. Fig. 3 shows TGA-DTA curves of the different carrier's assisted LSCM samples. The total weight loss was 0.97 mg in NTP assisted LSCM, 0.39 mg in oxalic acid assisted LSCM, and 0.77 mg in citric acid assisted LSCM from room temperature to 1300 ºC. The first weight loss is 0.32mg in NTP assisted LSCM in the temperature range 30 - 490 °C, whereas the first weight loss is 0.2 mg in the oxalic acid used LSCM in range 30 - 338 °C and the first weight loss is 0.25 mg in citric acid used LSCM in range 30 - 334 °C. The second weight loss is 0.9 mg in NTP used LSCM in the temperature range 490 - 822 °C, whereas the second weight loss is 0.42 mg in citric acid used LSCM in range 334 - 688°C. The second weight loss was attributed to the reaction between the residual nitrate and carriers after the decomposition of the precursor and subsequent combustion of organic components.

The morphologies of $La_{0.75}Sr_{0.25}Cr_{0.5}Mn_{0.5}O_{3-\delta}$ perovskite nanoparticles synthesized using different carriers by combustion method as examined with scanning electron microscopy are shown in Fig. 4. NTP-assisted LSCM shows many nanosized particles of spherical shape in the range 100 – 500 nm (Fig. 4a). The LSCM powders synthesized using oxalic acid and citric acid as carriers consist of uniform nanoparticles shwoing less agglomeration. The average particle size of the $La_{0.75}Sr_{0.25}Cr_{0.5}Mn_{0.5}O_{3-\delta}$ perovskite powders calcinated at 1200 ºC is about 50 - 500 nm (Fig. 4(a) and (b)). The small size $La_{0.75}Sr_{0.25}Cr_{0.5}Mn_{0.5}O_{3-\delta}$ perovskite nanoparticles are very active, small size is also beneficial for decreasing the fabrication temperature of the anode film and enhancing the catalytic properties.

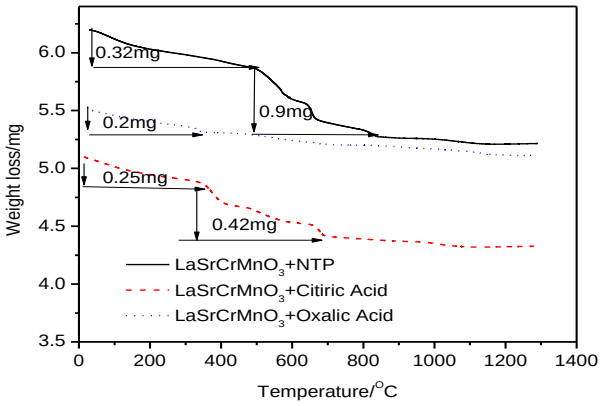

Figure 3: TGA curves of $La_{0.75}Sr_{0.25}Cr_{0.5}Mn_{0.5}O_{3-\delta}$ (LSCM) perovskite gel precursor dried at 120º C and then fired at 350 ºC for 1h.

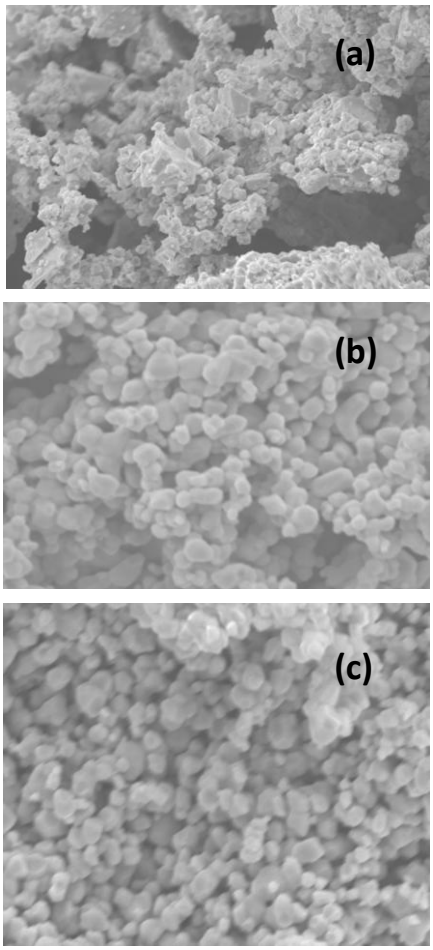

Figure 4: SEM images of $La_{0.75}Sr_{0.25}Cr_{0.5}Mn_{0.5}O_{3-\delta}$ perovskite phase nanoparticles (a) NTP-assisted, (b) oxalic acid assisted and (c) citric acid assisted.

4 CONCLUSIONS

$La_{0.75}Sr_{0.25}Cr_{0.5}Mn_{0.5}O_{3-\delta}$ (LSCM) perovskite phase nanoparticles were successfully synthesized by solution combustion method using different carriers (NTP, oxalic acid, and citric acid) after calcination of fired gel at 1200 ºC for 7 h. Scanning electron microscopy of the as-synthesized powders showed spherical particle shapes and sizes in the range of 50 – 500nm. An exothermic reaction between carriers and nitrates initiates the combustion process. TGA and DSC analysis confirmed the decomposition process of nitrates and the organic matter. The combustion reactions took place in the temperature range 200 ºC to 400 ºC.

ACKNOWLEDGEMENTS

One of the authors (V S Reddy Channu) thanks the Alexander von Humboldt Foundation for a fellowship.

REFERENCES

[1] Ch. Sun, U. Stimming, J. Power Sources 171 (2007) 247.
[2] E. Lay, G. Gauthier, S. Rosini, C. Savaniu, J.T.S. Irvine, Solid State Ionics 179 (2008)1562.
[3] S. Zha, P. Tsang, Z. Cheng, M. Liu, J. Solid State Chem. 178 (2005) 1844.
[4] S. Tao, J.T.S. Irvine, J. Electrochem. Soc. 151 (2) (2004) A252.
[5] S. TaO, J.T.S. Irvine, Nat. Mater. 2 (2003) 320.
[6] J.C. Ruiz-Morales, J. Canales-Vazquez, J. Pena-Martinez, D.M. Lopez, P. Nunez, Electrochim. Acta 52 (2006) 278.
[7] D.M. Bastidas, S. Tao, J.T.S. Irvine, J. Mater. Chem. 16 (2006) 1603.
[8] J. Wan, J.H. Zhu, J.B. Goodenough, Solid State Ionics 177 (2006) 1211.
[9] X.C. Lu, J.H. Zhu, Solid State Ionics 178 (2007) 1467.
[10] B. Huang, S. R. Wang, R.Z. Liu, X.F. Ye, H.W. Nie, X.F. Sun, T. L. Wen, J. Power Sources 167 (2007) 39.
[11] S.P. Jiang, X.J. Chen, S.H. Chan, J.T. Kwok, J. Electrochem. Soc. 153 (2006)A850.
[12] J. Pena-Martinez, D. Marrero-Lopez, J.C. Ruiz-Morales, B.E. Buergler, P. Nunez, L.J. Gauckler, J. Power Sources 159 (2006) 914.
[13] S.P. Jiang, X.J. Chen, S.H. Chan, J.T. Kwok, K.A. Khor, Solid State Ionics 177 (2006)149.
[14] J. Pena-Martinez, D. Marrero-Lopez, J.C. Ruiz-Morales, C. Savaniu, P.Nunez, J.T.S.Irvine, Chem. Mater. 18 (2006) 1001.
[15] J.C. Ruiz-Morales, J. Canales-Vazquez, B. Ballesteros-Perez, J. Pena-Martinez, D.Marrero-Lopez, J.T.S. Irvine, P. Nunez, J. Eur. Ceram. Soc. 27 (2007) 4223.
[16] S.P. Jiang, L. Zhang, Y. Zhang, J. Mater. Chem. 17 (2007) 2627.
[17] L. Zhang, S.P. Jiang, C.S. Cheng, Y. Zhang, J. Electrochem. Soc. 154 (2007) B577.
[18] S. B. Ha, P-S. Cho, Y. H. Cho, D. Lee, J.-H. Lee, J. Power Sources 195 (2010) 124.
[19] Z. Hu, Y. Yang, X. Shang, H. Pang, Mater. Lett. 59 (2005) 1373.
[20] K.C. Patila, S.T. Arunab, T. Mimania, Curr. Opin. Solid State Mater. Sci. 6 (2002)507.
[21] M.A. Raza, I.Z. Rahman, S. Beloshapkin, J. Alloys & Compd.485 (2009) 593.
[22] B. Liu, Y. Zhang, J. Alloys Compd. 453 (2008) 418.